

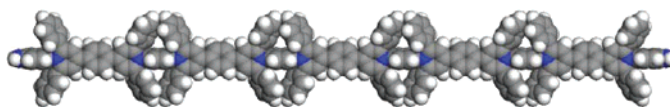
Oligomers of “Extended Viologen”, *p*-Phenylene-bis-4,4'-(1-aryl-2,6-diphenylpyridinium), as Candidates for Electron-Dopable Molecular Wires

Michal Valášek,^{†,‡} Jaroslav Pecka,^{*,†} Jindřich Jindřich,^{†,‡} Gérard Calleja,[†] Peter R. Craig,[†] and Josef Michl^{*,‡}

Department of Organic Chemistry, Charles University, Albertov 2030, Prague 2, Czech Republic, and
Department of Chemistry and Biochemistry, University of Colorado, Boulder, Colorado 80309-0215

michl@eefus.colorado.edu

Received May 20, 2004



We report the synthesis and spectral characterization of the first five members of an oligomeric series built from alternating *p*-connected 1,4-benzene and 1,4-pyridinium rings, **1[n]–4[n]**, $n = 1–5$, with *p*-phenylene-bis-4,4'-(1-aryl-2,6-diphenylpyridinium) (“extended viologen”) as the repeating unit. The lengths of these rodlike molecules range from 2 to 9 nm. The monomer was obtained from *p*-phenylene-bis-4,4'-(2,6-diphenylpyrylium) (**5**) and *p*-phenylenediamine (**6**) or *p*-aminoacetanilide (**9**). Higher oligomers were synthesized by stepwise elaboration of the monomer by reactions with the appropriate bis-pyrylium (**5**) or pyrylium-phenylene-pyridinium (**8**) salts. Eight different counterions were used, and dodecamethylcarba-*closo*-dodecaborate was found to offer particularly favorable solubility characteristics. Ultraviolet absorption spectra of the oligomers suggest that the individual extended viologen segments interact only weakly, as a result of the strongly twisted orientation of the benzene rings that separate them. The UV spectrum of the monomer was interpreted by comparison with semiempirical INDO/S calculations performed at a DFT optimized geometry.

It would be useful for molecular electronics to have several sets of linear and somewhat rigid molecules available in incremental lengths in the range of several nanometers that would be easily dopable with electrons but not with holes (i.e., easily reducible but not oxidizable). For the testing of theoretical notions¹ it would be particularly desirable for some of these “molecular *n*-semiconductor wires” to consist of well-defined somewhat insulated segments to serve as “rest stations” for an added electron, still permitting the electron to hop fairly rapidly from one segment to the next. This should yield wires whose conductivity drops only linearly and not exponentially with wire length. In long “wires”, when

such segmentation is not introduced intentionally, electron transfer will still proceed by polaron hopping, but the rest stations will be defined by random irregularities in wire conformation, adventitiously present ions, solvent inhomogeneities, etc. and will not be well controlled.

Ultimately, the ends of these wires are to be provided with functionalities that permit attachment to other structures, including metal electrodes, but for the moment, we merely wish the termini to contain functional groups that could be used as attachment points in the future. Many “molecular wires” have been reported before,^{2,3} but none seemed to meet our set of requirements.

We have chosen to examine the suitability of oligomeric structures **1[n]–4[n]** (Chart 1), where n stands for the

[†] Charles University.

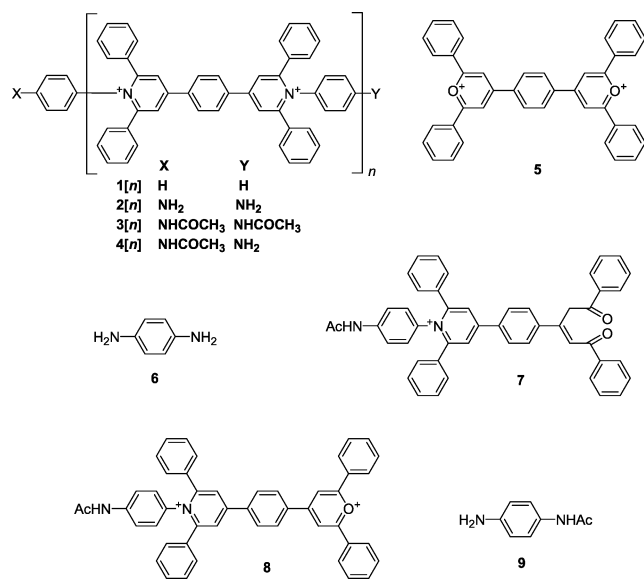
[‡] University of Colorado.

(1) Berlin, Y. A.; Hutchison, G. R.; Rempala, P.; Ratner, M. A.; Michl, J. *J. Phys. Chem. A* **2003**, *107*, 3970.

(2) Tour, J. M. *Chem. Rev.* **1996**, *96*, 537.

(3) Schwab, P. F. H.; Levin, M. D.; Michl, J. *Chem. Rev.* **1999**, *99*, 1863.

CHART 1



number of elementary segments in the molecule, and the terminal functionalities are amines or protected amines. Polymers of this type containing alternating benzene and pyridinium rings have been known for some time^{4,5} in the form of mixtures of linear chains with a wide distribution of lengths. They are obtained by condensation of the *p*-phenylene-bis-4,4'-(2,6-diphenylpyrylium) salt **5**^{6,7} with linear diamines such as *p*-phenylenediamine (**6**). Such condensation reactions of pyrylium salts with amines were first described nearly a century ago,⁸ and the effects of solvent and anion have since been studied in considerable detail.^{9–12} Although it has not been always formulated this way,¹³ natural segmentation of the alternating benzene-pyridinium sequence within the polymer chains **1–4** that separates them into relatively weakly interacting subunits can be expected to generate 1,4-phenylene-bis-4,4'-pyridinium moieties. For obvious reasons, we refer to this unit as “extended viologen”. These presumably well conjugated nearly planar three-ring segments of the chain are separated by benzene rings that must be strongly twisted out of the conjugation plane by steric interactions caused by the presence of phenyl substituents in the α positions of the pyridinium rings. Despite the interest in polymers of this type,^{3,4,12,14} the short oligomers **1[n]–4[n]** have apparently never been isolated and individually characterized. We now report the synthesis, solubility, and spectra of salts of pure monomers **1[1]–4[1]**, dimers **2[2]–4[2]**, trimers

2[3] and **3[3]**, tetramers **2[4]** and **3[4]**, and pentamers **2[5]** and **3[5]**, differing in terminal substitution. We have examined their salts with eight different anions and find that those of CB₁₁Me₁₂[–]^{15,16} hold particular promise for future studies of redox and other properties, since they are highly soluble in many solvents, including those of fairly low polarity.

The condensation of bifunctional components of type AA, such as **6**, and BB, such as **5**, by attachment of A to B, is a facile source of numerous important high polymers composed of the chains A[ABBA]_nA, B[BAAB]_nB, and [AABB]_n, with a molecular weight determined by the condensation yield. However, the synthesis of an oligomer A[ABBA]_nA of a particular well-defined length *n* represents an interesting general challenge. A brute-force approach would be to use an excess of AA relative to BB, perform an uncontrolled condensation, and separate the oligomers formed. The choice of reactant ratio and the effect of the chain on the reactivity of its terminal groups will then determine the distribution of chain lengths, such that a particular value of *n* will be favored, but in general many oligomers will be formed in significant amounts and their separation is likely to be hard. Instead, more or less complex group protection methods can be used to manipulate the reactivity of the terminal groups and direct the synthesis toward a particular oligomer. These may place much less demand on purification methods but consist of a larger number of reaction steps. Depending on the exact nature of A and B, on the number and amounts of oligomers desired, and on the availability and ease of separation procedures, a compromise between the simplest brute force procedure and the most complex totally directed synthesis of a particular oligomer needs to be chosen.

New approaches to the preparation of well defined π -conjugated oligomers have emerged in recent years.^{2,17,18} The most elegant and efficient way to prepare long-chain oligomers uses an iterative divergent/convergent strategy,^{19,20} illustrated in Figure 1.²¹ A batch of monomer material M, with inactive end groups X' and Y', is divided into two portions. In one portion, the end group X' is activated by conversion to X. In the second portion, Y' is activated by conversion to Y. The two portions are then combined to form the dimer X'MMY' with loss of XY. Because the same end groups that were present in the monomer are now present in the dimer, the procedure can be repeated with a doubling of molecular length at each iteration. The advantages of this approach are the rapid growth of molecular length (proportional to 2^{*m*}, where *m* is the number of iterations) and relatively easy separation

(4) Harris, F. W.; Chuang, C. K.; Huang, X.; Janimak, J. J.; Cheng, S. Z. D. *Polymer* **1994**, *35*, 4940.

(5) Huang, S. A. X.; Chuang, C. K.; Cheng, S. Z. D.; Harris, F. W. *Polymer* **2000**, *41*, 5001.

(6) Krivum, S. V.; Dorofeenko, G. N. *Khim. Geterosikl. Soedin.* **1966**, *2*, 656.

(7) Dimroth, K.; Reichardt, C. *Liebigs Ann. Chem.* **1969**, *727*, 93.

(8) Baeyer, A. *Ber. Dtsch. Chem. Ges.* **1910**, *43*, 2337.

(9) Katritzky, A. R.; Brownlee, R. T. C.; Musamarra, G. *Tetrahedron* **1980**, *36*, 1643.

(10) Katritzky, A. R.; Manzo, R. H.; Lloyd, J. M.; Patel, R. C. *Angew. Chem.* **1980**, *19*, 306.

(11) Katritzky, A. R.; Manzo, R. H. *J. Chem. Soc., Perkin Trans. 2* **1981**, 571.

(12) Katritzky, A. R.; Czerney, P. *Eur. J. Org. Chem.* **1998**, *3*, 2623.

(13) Makowski, M. P.; Mattice, W. L. *Polymer* **1993**, *34*, 1606.

(14) Lin, F.; Cheng, S. Z. D.; Harris, F. W. *Polymer* **2002**, *43*, 3421.

(15) King, B. T.; Janoušek, Z.; Grüner, B.; Trammel, M.; Noll, B. C.; Michl, J. *J. Am. Chem. Soc.* **1996**, *118*, 3313.

(16) King, B. T.; Zharov, I.; Michl, J. *Chem. Innov.* **2001**, *31*, 23.

(17) Müllen, K. *Pure Appl. Chem.* **1999**, *99*, 1863.

(18) Martin, R. M.; Diederich, F. *Angew. Chem., Int. Ed.* **1999**, *38*, 1350.

(19) The iterative doubling approach was first described by Whiting and later used by Moore. See: (a) Inger, E.; Paynter, O. I.; Simmonds, D. J.; Whiting, M. C. *J. Chem. Soc., Perkin Trans. 1* **1987**, 2447. (b) Bidd, I.; Kelly, D. J.; Ottey, O. I.; Paynter, O. I.; Simmonds, D. J.; Whiting, M. C. *J. Chem. Soc., Perkin Trans. 1* **1983**, 1369. (c) Zhang, J.; Moore, J. S.; Xu, Z.; Aguirre R. A. *J. Am. Chem. Soc.* **1992**, *114*, 2273. (d) Xu, Z.; Moore, J. S. *Angew. Chem., Int. Ed. Engl.* **1993**, *105*, 1394.

(20) Pearson, D. L.; Tour, J. M. *J. Org. Chem.* **1997**, *62*, 1376.

(21) Tour, J. M. *Molecular Electronics*; World Scientific Publishing Co.: River Edge, NJ, 2003.

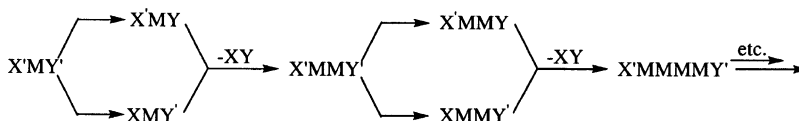
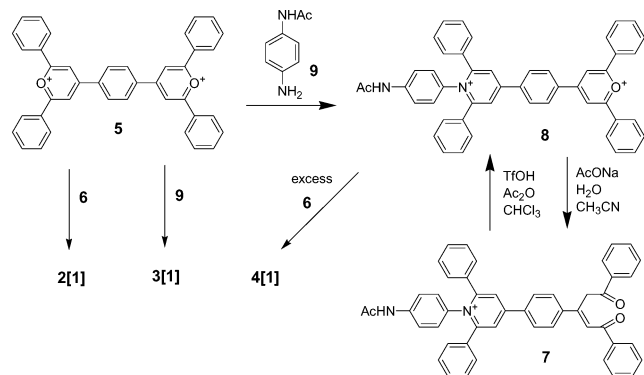


FIGURE 1. The iterative divergent/convergent approach to molecular wire length doubling.

SCHEME 1



of reaction products from unreacted material whose molecules are only half the size. The binomial strategy for oligomer preparation is also applicable to solid-phase synthesis,^{18,22} with the starting monomer or oligomer anchored covalently to an insoluble polymer resin.

Another possible strategy is the homo or hetero coupling of a symmetrical or asymmetrical monomer and eventual addition to the oligomerization mixture of an end-capping agent that irreversibly blocks the chain ends to prevent any further chain extension.^{23,24} This one-pot approach generally provides no control of oligoselectivity, and such a statistical polymerization often yields very low amounts of a particular oligomer. Nevertheless, this strategy can be useful in the absence of high yielding cross-coupling reactions, required in the iterative binomial synthesis, or if rapid access to an entire series of oligomers is desired and their chromatographic separations is feasible. Because the practical limit of this method is often dictated by difficulties encountered during the chromatographic separation of oligomers of similar molecular weight, it can be advantageous to perform the endcapping oligomerization reaction starting with higher oligomers.²⁵

Results and Discussion

In our particular case, AA = **6** and BB = **5**, several factors facilitate the synthesis: (i) We found that chromatography of PF₆⁻ salts on silica gel efficiently separates oligomers with *n* differing by unity, up to *n* = 4. (ii) The nucleophilic reactivity of the amino group in AA (**6**) far exceeds its reactivity in any oligomer A[ABBA]_{*n*}A or [AABB]_{*n*}, in which the aniline moiety is attached to the nitrogen of a pyridinium ring. This permits an exclusive transformation of a 2:1 molar ratio of AA (**6**) and BB (**5**) into AABBAA (**2[1]**), with negligible formation

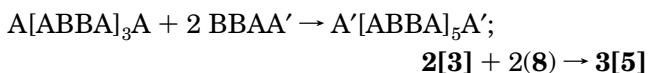
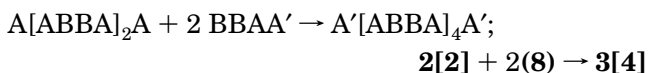
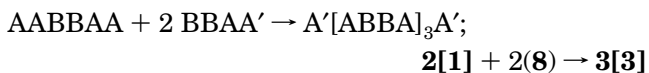
of the higher oligomers A[ABBA]_{*n*}A (**2[*n*]**), *n* > 1:



(iii) The amino group is easily reversibly protected by acetylation, and the pyrylium group is easily reversibly masked by hydrolysis to a 1,5-diketone. The half-protected monomer AA' (**4[1]**), the doubly protected structure A'ABB' (**7**), and the half-protected structure A'ABB (**8**) are all easily available:



Given these circumstances, we have elaborated reaction conditions for the following directed reaction sequences, and several of their variants:



Perchlorate, triflate, and tosylate salts were used most often. Tetrafluoroborate, trifluoroacetate, and chloride were used occasionally. Salts of the CB₁₁(CH₃)₁₂⁻ and PF₆⁻ anions were always prepared by exchange, as were some of the others. Perfluoropropionate was used in some of the HPLC separations.

Monomers [1] (Scheme 1). The dication **1[1]**, which has no terminal functional groups and will only be useful as a reference compound, was prepared readily from the trifluoromethanesulfonate salt of **5** and aniline. Salts of the terminally functionalized dications **2[1]** were prepared from **6** and the ClO₄⁻, CF₃SO₃⁻, *p*-MeC₆H₄SO₃⁻, BF₄⁻, and CF₃COO⁻ salts of **5**. As noted above, it is not necessary to use an excess of **6**. Salts of the bisacetamido derivative **3[1]** were prepared in an analogous fashion from **5** and **9**. They were also obtained by acetylation of the diamine salts **2[1]** with acetyl chloride. The hydrolysis of the diacetamide salt **3[1]** regenerates the diamine salts **2[1]**. Partial hydrolysis of the diacetamide **3[1]** can be directed to yield an about 50% yield of the monoacetamide **4[1]** in the reaction mixture, but the separation of **4[1]** from **2[1]** and unreacted **3[1]** is difficult and was only accomplished using HPLC.

A preferred route to **4[1]** uses the singly protected structure **8**, accessible from a condensation of excess triflate of **5** with **9**, followed by removal of **3[1]** and unreacted **5**. As a result of the instability of pyrylium salts during chromatographic separations, a practical method for isolation of compound **8** consists of quantitative hydrolysis of all pyrylium compounds in the reaction

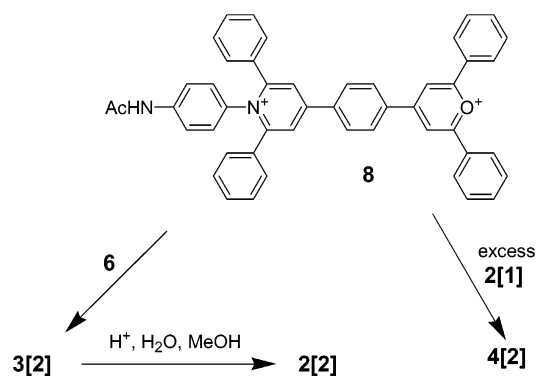
(22) Young, J. K.; Nelson, J. C.; Moore, J. S. *J. Am. Chem. Soc.* **1994**, *116*, 10841.

(23) Martin, R. E.; Gubler, U.; Boudon, C.; Gramlich, V.; Günter, P.; Gross, M.; Diederich F. *Chem. Eur. J.* **1997**, *3*, 1505.

(24) Altmann, M.; Enkelmann, V.; Beer, F.; Bunz, U. H. F. *Organometallics* **1996**, *15*, 394.

(25) Martin, R. E.; Mäder, T.; Diederich F. *Angew. Chem., Int. Ed.* **1999**, *38*, 817.

SCHEME 2



mixture using an aqueous sodium acetate, easy chromatographic separation of the corresponding unsaturated diketone **7**, and reformation of the original compound **8** using acetic anhydride and trifluoromethanesulfonic acid. Subsequent reaction of **8** with excess **6** yields **4[1]**, which can be purified by chromatography on silica gel using methanolic solution of KPF_6 as eluent.

Dimers [2] (Scheme 2). The best method for the synthesis of dimers is the reaction of 2 equiv of the monopyrylium salt **8** with **6**, which gives a high yield of **3[2]**. The diamine **2[2]** results from the hydrolysis of the diacetamide, and the aminoacetamide **4[2]** is produced by the reaction of the monopyrylium salt **8** with an excess of monomer **2[1]** followed by chromatography.

Trimers [3] (Scheme 3). The trimer **3[3]** is obtained by condensation of **5** with **4[1]** or by condensation of **8** with **2[1]**. Hydrolysis of the resulting diacetamide affords the diamine **2[3]**. Alternatively, **2[3]** is obtained by the condensation of **5** with a 50-fold excess of **2[1]**, followed by easy recovery of the unreacted diamine **2[1]** by extraction with a mixture of methanol and chloroform and by chromatography on a silica gel column using a solution of KPF_6 in acetonitrile/methanol mixtures as the eluent. This procedure appears awkward but is efficient for the preparation of large amounts. The recovered **2[1]** is recycled, and the overall yield is high.

Tetramers [4] (Scheme 4). The tetramer **3[4]** is prepared by the condensation of the diamine **2[2]** with 2

equiv of the monopyrylium salt **8**. Hydrolysis of the resulting diacetamide affords the diamine **2[4]**.

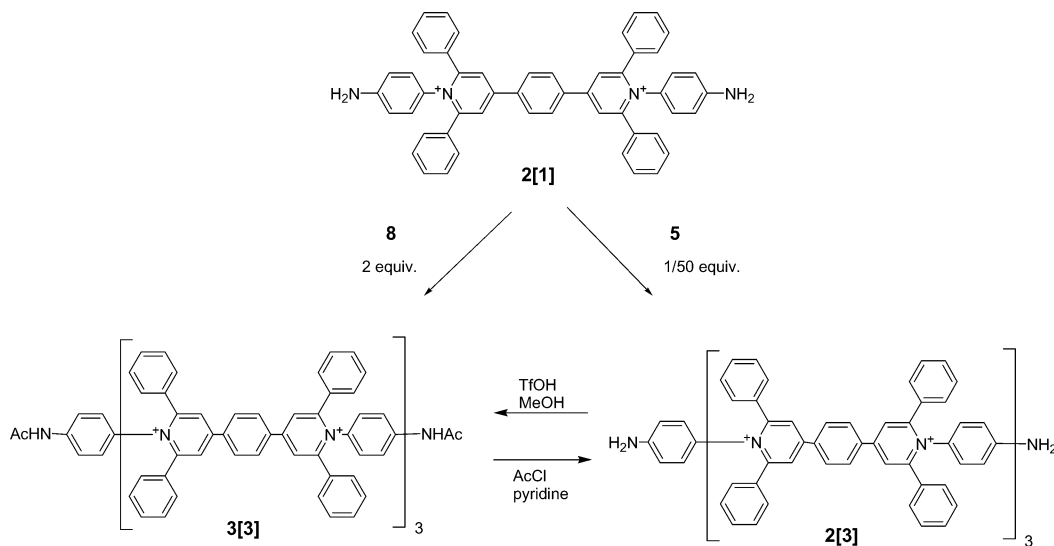
Pentamers [5] (Scheme 5). The pentamer **3[5]** is prepared by the reaction of the trimer **2[3]** with the monopyrylium **8**. In an alternative procedure, almost pure diacetamide **3[5]** resulted when the diamine **2[3]** was treated with an excess of the bispyrylium salt **5** and then an excess of **9**. The unreacted **5** was removed from the mixture by selective extraction with a methanol/chloroform mixture. The final purification was done by HPLC on a reversed-phase column using gradient methanol/water with ammonium pentafluoropropionate as the counterion.

The procedures given above are a result of an extensive investigation that examined several condensation schemes and various separation procedures: selective extraction, precipitation, and crystallization using solvent mixtures based primarily on methanol.

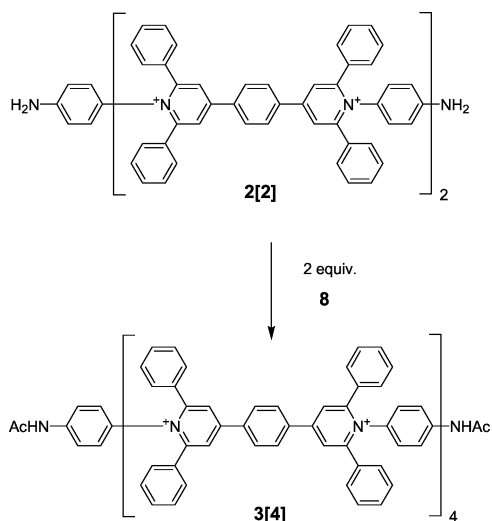
Considerable effort was devoted to optimizing column chromatography on silica, reversed-phase HPLC, and electrophoresis in $\text{DMF-H}_2\text{O}$ mixtures. The chromatography was complicated, conceivably as a result of aggregation of the charged chains of oligomers on the surface of the stationary phase or in solution at high concentrations, even in such polar solvents as acetonitrile or methanol. As mentioned below, we were unable to detect any aggregation in solution at spectroscopic concentrations, however. Problems with chromatographic separations were minimized when an excess of sorbents and ionic additives (CF_3COOH , $\text{C}_2\text{F}_5\text{COONH}_4$, KPF_6) dissolved in the mobile phase was used. The most suitable chromatographic method for the separation of low oligomers (up to the tetramer) used silica gel as a stationary phase and a solution of KPF_6 in methanol/acetonitrile mixtures as a mobile phase. The best separation resulted when all anions in the separated mixture of oligomers were first exchanged to PF_6^- .

Solubility. Insufficient solubility is frequently an issue when one deals with molecular wires and oligomers in general. We are using cationic oligomers in an effort to guarantee high reducibility and low oxidizability, and one of the side benefits is the freedom of choice of the

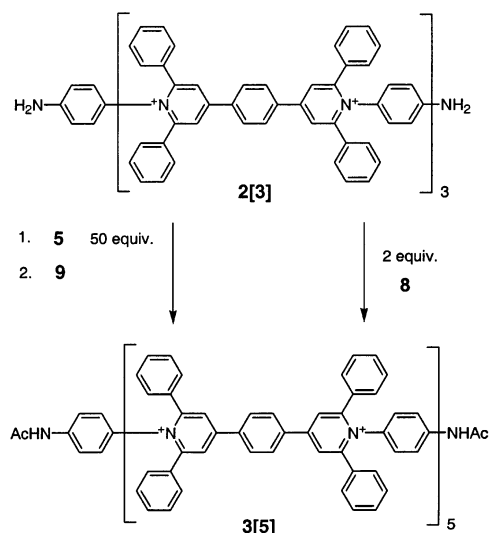
SCHEME 3



SCHEME 4



SCHEME 5

TABLE 1. Solubility of Salts of **3[1]** and **2[1]**^a

	methanol	acetonitrile	diethyl ether	chloroform
3[1] triflate	+	++	-	-
3[1] tosylate	+	++	-	+
3[1] ClO ₄ ⁻	+	++	-	-
3[1] CF ₃ COO ⁻	+	++	-	-
3[1] BF ₄ ⁻	+	++	-	-
3[1] CB ₁₁ Me ₁₂ ⁻	++	++	+	++
2[1] triflate	++	++	-	-
2[1] CB ₁₁ Me ₁₂ ⁻	++	++	++	++

^a ++ very soluble (>1 mM); + soluble (<1 mM); - insoluble.

counterion. Qualitative information about the solubilities of salts of several anions in selected polar and nonpolar solvents is provided in Table 1 for the monomers and in Table 2 for the oligomers. The high solubilizing power of the dodecamethylmonocarbocloso-dodecaborate anion^{14,15} CB₁₁Me₁₂⁻ is remarkable.

NMR Spectra. The degree of oligomerization *n* is apparent from integration of the ¹H NMR spectrum taken in DMSO-*d*₆, and integrated ¹H NMR spectra were used to judge the purity of the samples during the synthesis

TABLE 2. Solubility of **3[n]** Triflate and CB₁₁Me₁₂⁻ Salts^a

	3[n] -2 <i>n</i> (TfO ⁻)			3[n] -2 <i>n</i> (CB ₁₁ Me ₁₂ ⁻)		
	MeOH	MeCN	Et ₂ O	MeOH	MeCN	Et ₂ O
3[1]	+	++	-	++	++	+
3[2]	+	++	-	++	++	+
3[3]	-	+	-	++	++	+
3[4]	-	-	-	++	++	+
3[5]	-	-	-	++	++	+

^a ++ very soluble (>1 mM); + soluble (<1 mM); - insoluble.

TABLE 3. Number of Protons in Characteristic Regions in ¹H NMR Spectra of **2[n]**

H	δ							
	5.42	6.19–6.22	6.91–6.95	7.20–7.33	7.34–7.48	7.49–7.62	8.45–8.65	8.72
2[1]	4	4	4	16 <i>n</i> –16	20	8 <i>n</i> –8	8 <i>n</i> –4	4
2[2]	4	4	4	16	20	8	12	4
2[3]	4	4	4	32	20	16	20	4
2[4]	4	4	4	48	20	24	28	4
2[5]	4	4	4	64	20	32	36	4

TABLE 4. Number of Protons in Characteristic Regions in ¹H NMR Spectra of **3[n]**

H	δ						
	1.97	7.20–7.33	7.34–7.48	7.49–7.62	8.45–8.65	8.79	10.02
3[1]	6	16 <i>n</i> –8	20	8 <i>n</i> –8	8 <i>n</i> –4	4	2
3[2]	6	8	20	8	4	4	2
3[3]	6	24	20	8	12	4	2
3[4]	6	40	20	16	20	4	2
3[5]	6	56	20	24	28	4	2
3[5]	6	72	20	32	36	4	2

and purification process. We show the number of protons in the characteristic regions for diamine oligomers **2[n]** and diacetamido oligomers **3[n]** in Tables 3 and 4, respectively.

We have examined the temperature dependence of ¹H NMR spectra of salts of **3[1]** in a search for evidence of aggregation in solution. These measurements were performed on 10⁻³ to 10⁻⁵ M solutions of the triflate salt in DMSO-*d*₆ and of the CB₁₁Me₁₂⁻ salt in THF-*d*₈, and the spectra were found to be nearly temperature and concentration independent. Regular shifts to higher field by 0.1 ppm or less were observed for most peaks at elevated temperatures, except for the acetamido NH protons, whose peak shifted by about 0.25 ppm. We concluded that the spectra provide no evidence for aggregation at these concentrations.

¹³C NMR signals of **2[1]** and **3[1]** were assigned by DEPT, HMQC, and HMBC.

Mass Spectra. The observed molecular peaks (with and without an anion or anions, with multiple charge) served as a part of the structure proof. However, in general, mass spectra were not particularly helpful as an analytical tool during sample synthesis and purification of mixtures, and we relied on ¹H NMR spectra instead.

Molecular Structure. Possible future applications of the new molecular wires will be facilitated by reliable

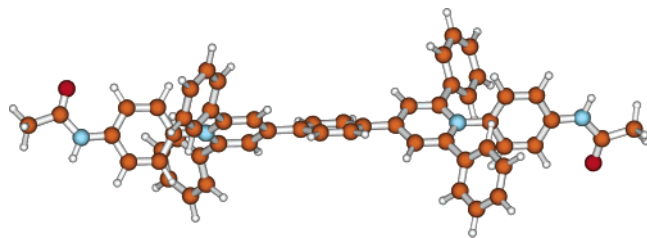


FIGURE 2. DFT optimized geometry of a conformer of **3[1]**.

information on their lengths. Unfortunately, all of our attempts to grow X-ray quality crystals failed. This may be related to the existence of a large number of conformers that are expected even in the first members of the series, **1[1]**–**4[1]**, and more so in the higher members. The three aromatic rings of the extended viologen unit are similar to those in *p*-terphenyl and can be expected to be only approximately coplanar in the ground state. The twists on the two sides of the central ring can be of the same handedness, in which case the central three-ring system has a 2-fold axis of symmetry passing through the middle ring, or of opposite handedness, in which case the central three-ring system has a plane of symmetry passing through the middle ring. Additional conformational freedom is associated with the inclination of the planes of the three terminal aryl substituents on each end of the extended viologen unit relative to the plane of the pyridinium ring to which they are all attached. If these aryls were twisted perpendicular to the pyridinium ring, there would be no conformational choices. However, the twist angles are almost certainly smaller than 90°, and there are four possibilities. In the first two, all three substituents can be twisted in the same sense, to the left or to the right. In the other two, the plane of the central aryl is aligned nearly exactly perpendicularly, one of the others to the left, and the other to the right. Preliminary calculations suggested that the numerous conformers that result from various combinations of the possibilities available to the central three rings of the extended viologens and to the three substituents on each end are comparable in energy, easily interconvertible, and not really different in the one parameter that is of most interest presently, the length of the molecular rod. We have therefore chosen one of the conformers of **3[1]** at random (C_2 symmetry, with 2-fold axis through the middle benzene ring and all three substituents on each end twisted in the same sense) and optimized its geometry using the B3LYP/6-31G(d) method (Figure 2).²⁶ This yielded a distance of 22.7 Å between the nitrogens of the two terminal acetamido groups. The increment for going to each next higher oligomer should be roughly equal to the distance between one of these nitrogen atoms and the distant pyridinium nitrogen, which is 17.0 Å. The estimated acetamido nitrogen to acetamido nitrogen distances in the **3[n]** rods therefore would be about 22.7, 39.7, 56.7, 73.7, and 90.7 Å for $n = 1$ –5, respectively, if the rod were perfectly straight.

The optimized twist angles in this conformer are ~35° on each side of the central benzene ring in the extended viologen structure, ~69° for the central acetamidophenyl substituent, and 54° and 58° for its two phenyl neighbors.

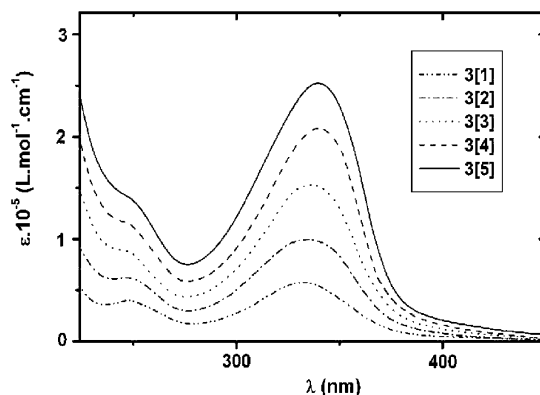


FIGURE 3. UV spectra of **3[n]** salts with $\text{Me}_{12}\text{CB}_{11}^-$ anions in acetonitrile.

TABLE 5. First Maximum in UV Absorption Spectra of Oligomers **3[n]**^a

	acetonitrile		THF	
	λ_{max}	$\epsilon \times 10^{-5}$	λ_{max}	$\epsilon \times 10^{-5}$
3[1]	331	0.53	337	0.52
3[2]	334	0.99	342	0.97
3[3]	337	1.52	345	1.49
3[4]	340	2.06	348	2.02
3[5]	342	2.52	351	2.48

^a Peak position λ_{max} in nm and decadic molar absorption coefficient ϵ in units of $\text{L mol}^{-1} \text{cm}^{-1}$ with an estimated accuracy of 3%.

Electronic Spectra. Similarly as the NMR spectra, ultraviolet spectra yielded no evidence for aggregation in solution. We found no deviations from the Lambert–Beer law for the $\text{CB}_{11}\text{Me}_{12}^-$ salt of **3[1]** in THF and DMSO in the range examined (10^{-4} to 10^{-8} M).

The spectra of the five oligomers **3[1]**–**3[5]** in acetonitrile are shown in Figure 3; those in THF are very similar (cf. Table 5). The spectra start with an indistinct tail that reaches into the visible region and contain a broad intense band with a maximum near 335 nm and a weaker less distinct band or shoulder near 250 nm. The strong ~335 nm band is shifted by only about 3 nm to the red in the spectrum of each successive oligomer, but the accuracy of this determination is low because the band is broad and the peak is ill-defined. The weak tail in the visible appears to be red-shifted upon wire length extension somewhat more strongly, whereas the position of the 250 nm band does not appear to be affected at all. The spectra of the five oligomers are thus nearly proportional to each other and confirm the segmentation of the oligomeric chain into very weakly interacting units, as anticipated from the calculated strong twists of the

(26) Frisch, M. J.; Trucks, G. W.; Schlegel, H. B.; Scuseria, G. E.; Robb, M. A.; Cheeseman, J. R.; Zakrzewski, V. G.; Montgomery, J. A., Jr.; Stratmann, R. E.; Burant, J. C.; Dapprich, S.; Millam, J. M.; Daniels, A. D.; Kudin, K. N.; Strain, M. C.; Farkas, O.; Tomasi, J.; Barone, V.; Cossi, M.; Cammi, R.; Mennucci, B.; Pomelli, C.; Adamo, C.; Clifford, S.; Ochterski, J.; Petersson, G. A.; Ayala, P. Y.; Cui, Q.; Morokuma, K.; Malick, D. K.; Rabuck, A. D.; Raghavachari, K.; Foresman, J. B.; Cioslowski, J.; Ortiz, J. V.; Stefanov, B. B.; Liu, G.; Liashenko, A.; Piskorz, P.; Komaromi, I.; Gomperts, R.; Martin, R. L.; Fox, D. J.; Keith, T.; Al-Laham, M. A.; Peng, C. Y.; Nanayakkara, A.; Gonzalez, C.; Challacombe, M.; Gill, P. M. W.; Johnson, B. G.; Chen, W.; Wong, M. W.; Andres, J. L.; Head-Gordon, M.; Replogle, E. S.; Pople, J. A. *Gaussian 98*, revision A.9; Gaussian, Inc.: Pittsburgh, PA, 1998.

TABLE 6. Results of INDO/S²⁶ Calculations for a C₂-Symmetry Conformer of **3[1]**

no.	energy ^a	λ^b	f^c	sym	pol ^d	leading configurations
1	24.5	408	0.00005	A	<i>z</i>	2 → -1, 1 → -2
2	24.5	408	0.0012	B	<i>x</i>	1 → -1, 2 → -2
3	30.3	330	0.12	B	<i>y</i>	3 → -1, 4 → -2
4	30.4	329	0.56	A	<i>z</i>	4 → -1, 3 → -2
5	33.6	298	0.0006	B	<i>x</i>	2 → -4, 1 → -3
6	33.6	298	0.009	A	<i>z</i>	2 → -3, 1 → -4
7	34.2	293	0.43	B	<i>x</i>	7 → -1, 8 → -2
8	35.1	285	0.0002	A	<i>z</i>	8 → -1, 7 → -2, ...
9	36.3	275	0.12	B	<i>x</i> (y) ^e	9 → -1, 10 → -2, ...
10	36.4	275	0.001	A	<i>z</i>	12 → -1, 11 → -2
11	36.4	274	0.11	B	<i>x</i> (y) ^e	11 → -1, 12 → -2
12	36.8	272	0.00002	A	<i>z</i>	10 → -1, 9 → -2, 7 → -2, 8 → -1
13	37.7	265	0.045	B	<i>x</i>	2 → -2, 1 → -1
14	37.7	265	0.00007	A	<i>z</i>	1 → -2, 2 → -1
15	39.1	256	0.69	B	<i>x</i>	2 → -7, 1 → -8
16	39.1	256	0.0004	A	<i>z</i>	1 → -7, 2 → -8
17	39.7	252	0.011	A	<i>z</i>	2 → -10, 1 → -9
18	39.7	252	0.15	B	<i>y</i>	1 → -10, 2 → -9
19	40.2	249	0.24	B	<i>x</i>	4 → -4, 3 → -3
20	40.3	248	0.00001	A	<i>z</i>	3 → -4, 4 → -3
21	41.1	243	0.0057	B	<i>x</i>	5 → -1, 6 → -2
22	41.2	243	0.0005	A	<i>z</i>	6 → -1, 5 → -2
23	43.0	232	0.16	B	<i>y</i>	7 → -3, 8 → -4, 3 → -1, ...
24	43.1	232	0.075	A	<i>z</i>	7 → -4, 8 → -3, 4 → -1, ...
25	43.9	228	0.12	B	<i>x</i>	11 → -3, 12 → -4, 2 → -11, 1 → -12
26	43.9	228	0.00000	A	<i>z</i>	1 → -11, 12 → -3, 11 → -5, 2 → -12, ...
27	44.2	226	0.0002	A	<i>z</i>	3 → -2, 4 → -1, ...
28	44.2	226	0.14	B	<i>y</i>	4 → -2, 3 → -1, ...
29	44.7	224	0.0004	B	<i>y</i>	2 → -11, 1 → -12, 11 → -3, 12 → -4, ...
30	44.8	223	0.0009	A	<i>z</i>	1 → -11, 2 → -12, 12 → -3, 11 → -4, ...
31	45.1	222	0.002	A	<i>z</i>	7 → -4, 8 → -3, ...
32	45.1	222	0.098	B	<i>y</i>	7 → -3, 8 → -4, 10 → -4, 9 → -3, ...
33	46.0	217	0.00005	A	<i>z</i>	8 → -1, 7 → -2
34	46.6	215	0.029	B	<i>x</i>	8 → -2
35	47.1	212	0.00010	B	<i>x</i>	6 → -7, 5 → -8
36	47.1	212	0.0001	A	<i>z</i>	5 → -7, 6 → -8
37	47.3	212	0.00003	B	<i>y</i>	1 → -3, 2 → -4
38	47.3	211	0.00008	A	<i>z</i>	2 → -3, 1 → -4
39	47.8	209	0.00000	B	<i>y</i>	2 → -6
40	47.8	209	0.002	A	<i>z</i>	1 → -6

^a Excitation energy in 10³ cm⁻¹. ^b Wavelength in nm. ^c Oscillator strength from the mixed dipole length-dipole velocity formula.

^d The 2-fold symmetry axis is *z* and the long axis is *x*. ^e The polarization direction deviates significantly from *x* toward *y*.

planes of the benzene rings that separate the individual extended viologens. The weak tail at long wavelengths suggests the presence of one or more very weakly allowed transitions at low energy, and this is compatible with our failure to detect any fluorescence.

To provide an interpretation of the absorption spectrum of the extended viologen chromophore, we performed an INDO/S²⁷ calculation at the optimized geometry of **3[1]** described above. The results depended only slightly on the extent of configuration interaction used. Table 6 lists the data obtained for the low energy transitions with single excitations from the 12 highest occupied to the 12 lowest unoccupied orbitals. State symmetries refer to the C₂ group, *z* is the symmetry axis, *y* is the out-of-plane axis at the central benzene ring, and *x* is the long axis of the molecule. Transitions into states of A symmetry are polarized along *z*, and those into states

of B symmetry are marked with *x* or *y* in Table 6 to indicate the approximate polarization direction.

The molecular orbitals occupied in the ground state are labeled 1, 2, 3, ... starting with the highest energy one (HOMO), and those unoccupied in the ground state are labeled -1, -2, -3, ... starting with the lowest energy one (LUMO). Only six occupied (1, 2, 3, 4, 7, 8) and four unoccupied (-1, -2, -7, -8) orbitals are involved in excitations that are believed to be detectable in the UV spectrum. All of them can be described as combinations of the frontier molecular orbitals of a substituted benzene ring. In addition to the nodal plane common to all p orbitals, the two highest occupied benzene π orbitals have only one additional nodal plane. This cuts through the position of substitution (1) in one of the benzene HOMOs (A) and cuts across bonds 2-3 and 5-6 in the other (S). Its two lowest unoccupied π orbitals have two additional nodal planes, one of which cuts through position 1 and the other through bonds 2-3 and 5-6 in orbital -A, and both of which cut through bonds (1-2, 4-5 and 3-4, 1-6) in orbital -S.

Arguably -1 is the most interesting orbital in **3[1]**. It is the lowest unoccupied orbital (LUMO), the one that will accept an electron when the molecular wire is doped. This orbital is antisymmetric (b) with respect to rotation about the 2-fold symmetry axis and is almost entirely concentrated on the central three-ring system. It is most easily described as an in-phase combination of the -S orbitals on each of the three rings. Orbital -2 (a), calculated to be about 0.5 eV higher in energy, is the antisymmetric combination of the -S orbitals on the pyridinium rings and has a very small amplitude on the central ring. The virtual orbitals -1 and -2 play an essential role in the UV spectra discussed below, because they serve as the terminating orbitals of almost all the important transitions. The only other two important antibonding orbitals of **3[1]** are -7 (a) and -8 (b), which are located another 1.8 eV higher in energy. They represent the in-phase and out-of-phase combinations of the -S orbitals of the two terminal acetamidophenyl groups that are twisted nearly perpendicular to the plane of the three central rings. This orthogonality and spatial separation are responsible for an almost complete absence of any interaction between the terminal rings, and as a result the orbitals -7 and -8 are almost exactly degenerate.

The HOMO orbitals of **3[1]**, 1 (a) and 2 (b), are also nearly exactly degenerate, for the same reason. They are the in-phase and out-of-phase combinations of the S orbitals of the two terminal twisted acetamidophenyl groups, with strong antibonding participation by the acetamido nitrogen lone pairs, which contributes to the relatively high orbital energy. About 1 eV lower in energy are the orbitals 3 (a) and 4 (b), again nearly exactly degenerate, for a similar reason. These orbitals are formed by the out-of-phase and in-phase combinations of the A orbitals on the two pyridinium rings. The A orbitals again cannot interact, although the three rings are only partially twisted, because they are connected through atoms at which they have a node. Each of these A orbitals is, however, delocalized onto the two phenyl substituents carried by the pyridinium ring and to a smaller degree also onto the acetamidophenyl substituent. The last important set are orbitals 7 (a) and 8 (b),

(27) Ridley, J.; Zerner, M. C. *Theor. Chim. Acta* **1973**, *32*, 111.

located ~ 0.2 and ~ 0.3 eV further down in energy. These are the in-phase and out-of-phase combination of the acetamido nitrogen lone pairs delocalized significantly onto all three aryl substituents carried by the pyridinium ring. Orbital 7 also contains a large contribution from the S orbital of the middle benzene ring.

As would be expected for a molecule of this size, theory predicts a very large number of singlet–singlet transitions in the low-energy region of the spectrum (Table 6). The compartmentalization of the molecular orbitals into the central three-ring system on one hand and a pair of mutually only weakly interacting sets of three twisted aryl substituents on the pyridinium rings on the other hand has two important consequences for the UV spectra. First, many transitions are nearly exactly doubly degenerate, and second, only very few are strongly allowed, permitting a facile comparison with the observed spectrum.

The transitions into the two lowest energy states, one of A symmetry ($1 \rightarrow -2$ and $2 \rightarrow -1$, z polarization) and one of B symmetry ($1 \rightarrow -1$ and $2 \rightarrow -2$, x polarization), are both calculated at 408 nm. They have equal energies because they correspond to electron transfer from the nearly degenerate pair of HOMOs located on the extremely weakly interacting terminal acetamidophenyl rings to the central three-ring system. Like the many other calculated transitions that transfer an electron between orbitals that are entirely separated in space, they have no significant oscillator strength. We suggest that these transitions are responsible for the weak absorption tail observed at the edge of the visible region. Their small transition moment causes the fluorescence rate constant to be small, too, providing an excellent opportunity for other processes, such as intersystem crossing or internal conversion, to compete successfully with fluorescence, which is indeed not observed.

The next pair of calculated transitions carries large oscillator strength, occurs near 330 nm, and is again nearly degenerate. The weaker of the excitations is polarized along y (B state, $3 \rightarrow -1$ and $4 \rightarrow -2$) and the stronger one along z (A state, $4 \rightarrow -1$ and $3 \rightarrow -2$); together they account for the prominent absorption band observed near 335 nm. These transitions are localized in the two substituted pyridinium rings and involve A to $-S$ excitations reminiscent of the B_{2u} transition in benzene. It is perhaps counterintuitive that the first intense band in the spectrum of a rod-shaped molecule should not be long axis polarized. Other such cases are known (polyacenes), but it would be worth the effort to check this experimentally. The next intense transition is into a state of B symmetry, is predicted to be long axis (x) polarized, and to occur at 293 nm. It is due to a superposition of $7 \rightarrow -1$ and $8 \rightarrow -2$ electron promotions, and its intensity seems to originate from the S to $-S$ excitation in the middle benzene ring. There is no separate spectral peak at this wavelength, but the spectral envelope of the 335 nm band is so broad that it is easy to believe that the transition calculated at 293 nm is present and contributes to this massive band. We

therefore propose that the three transitions together account for the broad and intense absorption feature observed near 335 nm. An experimental verification of this interpretation would be possible using polarization spectroscopy.

The next calculated transition that carries significant intensity is located at 256 nm. The excited state is of B symmetry, the transition is long-axis (x) polarized, and is due to a combination of electron promotions $2 \rightarrow -7$ and $1 \rightarrow -8$. This corresponds to an S to $-S$ excitation in the terminal acetanilide rings, analogous to the B_{1u} transition in acetanilide itself. This transition is readily assignable to the absorption band observed at ~ 250 nm.

Overall, then, the calculations for the conformer shown in Figure 2 account nearly perfectly for the observed absorption spectrum of **3[1]** and make some definite, unexpected, and verifiable transition polarization predictions. We believe that the spectra of the numerous other anticipated low-energy conformers would be similar.

Summary

We have prepared and characterized five lengths of a molecular wire suitable for doping with electrons but not likely to accept holes, ranging from 2 to 9 nm. The structures are of a type previously known from polymer chemistry and consist of alternating benzene and pyridinium rings. They carry terminal amino groups, meant to permit future functionalization appropriate for attachment to surfaces or to other molecular building blocks. When the inert and lipophilic $CB_{11}Me_{12}^-$ counterion is used, even the largest polycations studied (250 carbon atoms) are soluble, also in solvents of only moderate polarity.

The wires are structurally segmented into 1–5 weakly interacting subunits of the extended viologen type by the presence of strongly twisted benzene rings. The subunits are expected to function as sojourn stations within which an added electron can be temporarily delocalized as it hops from one subunit to the next. The shortest wire, which consists of only one extended viologen subunit, has been examined in detail. At concentrations of 10^{-3} M and lower, there is no sign of aggregation in solution. Three characteristic features of the electronic absorption spectrum, a tail reaching into the visible region and two bands in the ultraviolet, have been interpreted by comparison with INDO/S calculations.

Acknowledgment. We are grateful to Dr. Pawel Rempala and Mr. Gregg Kottas for help with the computations and to the Grant Agency of Czech Republic (GACR 203/01/0644), DARPA/ONR (N00014-99-1-0474) and the National Science Foundation (CHE-0140478) for support.

Supporting Information Available: Experimental details. This material is available free of charge via the Internet at <http://pubs.acs.org>.

JO049142S